Xenobiotica
the fate of foreign compounds in biological systems

ISSN: (Print) (Online) Journal homepage: www.tandfonline.com/journals/ixen20

Human keratinocyte response to 4,4'-methylene diphenyl diisocyanate-glutathione conjugate exposure

Brandon F. Law, Chen-Chung Lin & Justin M. Hettick

To cite this article: Brandon F. Law, Chen-Chung Lin & Justin M. Hettick (2024) Human keratinocyte response to 4,4'-methylene diphenyl diisocyanate-glutathione conjugate exposure, Xenobiotica, 54:9, 749-758, DOI: 10.1080/00498254.2024.2401493

To link to this article: https://doi.org/10.1080/00498254.2024.2401493

XENOBIOTICA
2024, VOL. 54, NO. 9, 749–758
https://doi.org/10.1080/00498254.2024.2401493

Taylor & Francis
Taylor & Francis Group

RESEARCH ARTICLE

Human keratinocyte response to 4,4′-methylene diphenyl diisocyanate-glutathione conjugate exposure

Brandon F. Law, Chen-Chung Lin and Justin M. Hettick

Allergy and Clinical Immunology Branch, Health Effects Laboratory Division, National Institute for Occupational Safety and Health, Morgantown, WV, USA

ABSTRACT

1. Workplace exposure to diisocyanates like 4,4′-methylene diphenyl diisocyanate can cause occupational asthma (MDI-OA), and the underlying biological pathways are still being researched.
2. Although uncertainty remains, evidence supports the hypothesis that dermal exposure to MDI plays an important role in the development of MDI-OA.
3. Gene expression, proteomics, and informatics tools were utilised to characterise changes in expression of RNA and protein in cultured human HEKa keratinocyte cells following exposure to conjugates of MDI with glutathione (MDI-GSH).
4. RT-qPCR analysis using a panel of 39 candidate primers demonstrated 9 candidate genes upregulated and 30 unchanged.
5. HPLC-MS/MS analysis of HEKa cell lysate identified 18540 proteins across all samples 60 proteins demonstrate statistically significant differential expression in exposed cells, some of which suggest activation of immune and inflammatory pathways.
6. The results support the hypothesis that dermal exposures have the potential to play an important role in the development of MDI-OA. Furthermore, proteomic and gene expression data suggest multiple immune (adaptive and innate) and inflammatory pathways may be involved in the development of MDI-OA.

ARTICLE HISTORY
Received 13 June 2024
Revised 29 August 2024
Accepted 3 September 2024

KEYWORDS
4′-methylene diphenyl diisocyanate (MDI); human keratinocytes; occupational asthma (OA); label-free quantitative proteomics; isocyanates

Introduction

Diisocyanates are low molecular weight compounds used in the manufacture of diverse polyurethane products including foams, sealants, paints, adhesives, elastomers, insulating products and more. Global demand for 4,4′-methylene diphenyl diisocyanate (MDI, the most widely utilised diisocyanate) is reportedly 8.25 million metric tons and is expected to maintain a compound annual growth rate of > 5% (Intelligence 2023). Workplace exposure to MDI is one of the foremost causes of occupational asthma (OA) and occurs across a range of industries (DI Bernstein et al. 1993; NIOSH 1994a; NIOSH 1994b; Redlich and Karol 2002; Lofgren et al. 2003; Engfeldt et al. 2013; Wisnewski et al. 2022). OA is the most prevalent occupational respiratory disease in the United States and accounts for 9-15% of asthmatic patients at a cost to the US economy of billions of dollars annually (Blanc and Toren 1999; Balmes et al. 2003). Early diagnosis and identification of the causative agent is critical due to the medical and socioeconomic impact of OA (IL Bernstein 1999; Dewitte et al. 1994).

The *in vivo* biological fate of diisocyanates, such as MDI, post-exposure is debated, and the clinical presentation of patients is diverse. In general, patients don't experience asthma symptoms after the first exposure; rather, OA develops over months or years (Malo and Chan-Yeung 2009). This latent phase is common with environmental asthmas and reflects the sensitisation period typical of an allergic process (Maestrelli et al. 2009). However, diisocyanates can disrupt oxidative homeostasis leading to non-immunologic mechanisms and to the development of OA (Bowler and Crapo 2002; Rahman and MacNee 2002; Janssen-Heininger et al. 2009). To date, the specific biological mechanism(s) involved in the development of MDI-OA remain a recognised knowledge gap. Although MDI-OA shares similarities to allergic asthma, the majority of those diagnosed lack MDI-specific IgE (Wass and Belin 1989; Ye et al. 2006; Wisnewski et al. 2004), thus failing to meet to the classic definition of Type I Immune Hypersensitivity. Although alternative mechanisms including oxidative stress and chemical-induced toxicity have been explored (Wisnewski et al. 2002; CT Lee et al. 2005), no one definition or set of circumstances seems to indicate a predominant mechanism underlying the development of MDI-OA. It has been reported that as many as 100 genes may be associated with the development of asthma (Lambrecht and Hammad 2015). It is therefore possible, if not probable, that MDI-OA is a heterogenous condition with underlying mechanisms defined by individual genotypic and phenotypic differences.

CONTACT Brandon F. Law bhl7@cdc.gov Allergy and Clinical Immunology Branch, Health Effects Laboratory Division, National Institute for Occupational Safety and Health, 1095 Willowdale Rd., MS L4020, Morgantown, WV 26505, USA

Supplemental data for this article can be accessed online at https://doi.org/10.1080/00498254.2024.2401493.

Inhalation was long considered the primary exposure route for diisocyanates; this has, in part, driven industry to embrace MDI over more volatile diisocyanates such as toluene diioscyanate (TDI) and hexamethylene diisocyanate (HDI). Despite air monitoring data demonstrating workplace airborne MDI concentrations are generally well controlled and low to non-detectable (Booth et al. 2009), biomonitoring for MDI exposure in workers continues to indicate ongoing exposure, suggestive of a role in OA pathogenesis for dermal exposure. The skin, or more accurately, the dermal barrier, is key in protecting the human body from the external environment. The epidermis is the first line of defense for the host and primarily consists of keratinocytes which form a selectively permeable barrier between humans and the environment. In addition to keratinocytes, there exist a host of other cells, including professional immune cells, to monitor for antigens or signals indicating damage or infection (Yousef et al. 2024). Keratinocytes play an essential role in innate immune actions and participate in the activation of adaptive immune mechanisms (J-N Wang and Li 2020). Keratinocytes can detect both specific and non-specific threats and produce pro-inflammatory cytokines, alarmins, and process/present antigens to initiate actions against these threats (Piipponen et al. 2020; Chieosilapatham et al. 2021; Jiang et al. 2020). The epidermal barrier and immune responses are determined by downstream events related to cytokines, chemokines, and alarmins released by the assault. These downstream events lead to multiple effects including immune cell recruitment, antigen presentation, barrier repair, apoptosis, etc. It is possible that dermal MDI exposure may lead to downstream effects such as inflammation or immune memory, among other potential outcomes. If dermal exposure plays a key role in the development of MDI-OA, it stands to reason that keratinocytes can trigger and/or participate in immune reactions and other downstream events involved. Keratinocytes are a logical cell type to select when considering biological MDI exposure events, evidence of dermal exposures, the structure of the dermis, and their role in other immune responses.

This report utilises gene expression data in conjunction with bottom-up proteomics to elucidate potential early biological pathways related to MDI exposure in an *in vitro* keratinocyte cell culture model. Human keratinocytes were exposed to MDI as MDI-glutathione (GSH) conjugate. Glutathione is a key antioxidant and has been previously determined to be a primary target for isocyanates (dNCO) *in vivo* (Wisnewski et al. 2022). Furthermore, the use of MDI-GSH conjugate to dose cultured cells results in dramatically reduced cytotoxicity compared to dosing with free MDI. We hypothesise that exposure to the physiologically relevant MDI-GSH conjugate will improve cellular uptake of MDI and provide insights on pathways involved when epidermal barrier cells are exposed to MDI.

Materials and methods

Safety statement

4,4′-methylene diphenyl diisocyanate (MDI) is a hazardous chemical that requires strict safety precautions during handling and use. MDI is known to be a potent sensitiser and irritant. To ensure the safety of personnel, all work involving MDI was conducted in a well-ventilated fume hood to prevent inhalation of dust. Researchers wore appropriate personal protective equipment (PPE) including chemical-resistant gloves, safety goggles, and lab coats. In addition, a N95 respirator was used when handling large quantities of MDI or in cases where exposure risk was high. All waste containing MDI was disposed of in accordance with institutional and governmental regulations for hazardous waste. Emergency procedures were established and reviewed prior to the initiation of experiments to address potential exposure or spill incidents.

Chemicals and reagents

High performance liquid chromatography (HPLC) grade acetone, 3 Å molecular sieves (4–8 mesh), porcine trypsin, ammonium carbonate, ammonium formate, 98% 4,4′-methylene diphenyl diisocyanate (MDI) and reduced glutathione (GSH) were acquired from MilliporeSigma (St. Louis, MO). Dermal cell basal medium and keratinocyte growth kit were acquired from American Type Culture Collection (Manassas, VA). Dry acetone was prepared by incubating 10 mL HPLC grade acetone on 3 Å molecular sieves for a minimum of 24 h to adsorb water.

Cell culture

Cell cultures were established on two separate timepoints for a total $N=2$ with four technical replicates per sample group. Primary human epidermal keratinocytes (HEKa) (ATCC PCS-200-011) cells were obtained from American Type and Culture Collection (ATCC; Manassas, VA) and seeded into 100-mm cell culture dishes at 1.0×10^5 viable cells and grown in serum-free conditions using dermal cell basal media with keratinocyte growth kit supplements and 100 µg/mL and 100 U/mL of penicillin/streptavidin at 37 °C, 95% Rh in 5% CO_2. All experiments were performed from cells obtained from a single vial. Cells were sub-cultured at a rate of 1:4 once cultures reached 70-80% confluence by visual inspection. Sub-cultures were seeded using 1.0×10^5 viable cells as determined using trypan blue staining and a Countess 3 automated cell counter (Invitrogen, Carlsbad, CA). Media was changed every 48-h. At passage, four cells were allowed to reach near 100% confluence by visual inspection and exposed.

MDI-GSH conjugation, exposure, and validation

Exposure concentration (dose) and time were determined empirically based on observations of cytotoxicity. The dose selected elicited no obvious cytotoxic response using qualitative observations of cell health such as attachment and cell death/viability. It is not known if this exposure paradigm reflects what a worker may experience due to the knowledge gap with regards to real occupational dermal exposure and the diversity of the industries that utilise MDI. MDI-GSH conjugate was prepared as previously

described (Wisnewski et al. 2013). Briefly, a 10 mM GSH solution was prepared in complete keratinocyte growth medium (KGM). A 50 µL aliquot of freshly prepared 10% MDI (w/v) stock solution in dry acetone was added to 25 mL of 10 mM GSH solution/complete KGM dropwise with stirring to a final MDI concentration of 800 µM, after which the tube was subjected to gentle agitation for 2 h at 37 °C. Conjugates were centrifuged at 10 000 × *g* and filtered with a 0.2 µm syringe filter. MDI-GSH conjugate was prepared immediately before treatment. 10 mL of 100 µM MDI-GSH (exposed) or GSH only (control) was added to each culture, eight controls and nine exposed. After 24 h, the cell culture supernatant (conditioned media) was collected, centrifuged, and stored at −80 ° for undetermined future experiments. Cells were collected by mechanical scraping in 1 mL PBS and pelleted using centrifugation at 300 × *g* for 5-min. at 4 °C. MDI-GSH conjugate formation was validated using positive mode mass spectrometry.

Cell lysis and digestion

GSH-MDI exposed HEKa cells were collected and washed twice with cold PBS prior to lysis *via* three rapid freeze-thaw cycles followed by pressure gradient lysis using a Barocylcer 2320EXT (Pressure BioSciences, Inc., Medford, MA). at 37 °C, 50 cycles alternating between high (50 kpsi, 50 sec) and ambient pressure for 10 sec. Lysed cells were quantified for protein concentration using a Qubit 4 fluorometer (ThermoFisher Scientific, Waltham, MA) and diluted to 75 µg total protein per sample in 50 mM ammonium bicarbonate. Trypsin digestion (40:1 wt:wt) was performed at 37 °C utilising 50 cycles of alternating high (20 kpsi, 50 sec) and ambient pressure (10 sec) using the Barocycler.

Gene expression

Gene expression was determined by RT-qPCR analysis. Total RNA from cultured HEKa cells (4 exposed cultures and 4 non-exposed controls) was extracted using *mirVana*™ miR Isolation Kit (ThermoFisher Scientific) as per manufacturer's instructions. The mRNA levels were determined as previously described (Lin et al. 2011). Candidate gene expression was normalised to human beta-2 microglobulin (*B2M*) for mRNA analysis. Gene expression assays used in this study were obtained from ThermoFisher Scientific (Waltham, MA) and include: *CCL2* (Hs00234140_m1), *CCL3* (Hs00234142_m1), *CCL5* (Hs00982282_m1), *CCL11* (Hs00237013_m1), *CCL17* (Hs00171074_m1), *CCL22* (Hs01574247_m1), *CCL24* (Hs00171082_m1), *IL1b* (Hs01555410_m1), *IL2* (Hs00174114_m1), *IL4* (Hs00174122_m1), *IL5 (Hs01548712_g1), IL6 (Hs00174131_m1), IL8 (Hs00174103_m1), IL10 (Hs00961622_m1), IL12B (Hs01011518_m1), IL13 (Hs00174379_m1), IL17A (Hs00174383_m1), IL25 (Hs03044841_m1), IL33 (Hs04931857_m1), IFNG (Hs99999041_m1), TNF* (Hs00174128_m1), *TSLP (Hs00263639_m1), CXCL10 (Hs00171042_m1), TGFB1 (Hs00998133_m1), GMCSF (Hs00929873_m1), COX1 (Hs00377726_m1), COX2 (Hs00153133_m1), KLF4 (Hs00358836_m1), CEBPB (Hs00942496_s1), IRF4 (Hs00180031_m1), STAT6 (Hs00180031_m1), PPARg (Hs00608254_m1), SPI1 (Hs02786711_m1), HMGB1 (Hs01923466_g1), MCPIP (Hs00962356_m1), PPP3CA (Hs00174223_m1), NFATc2 (Hs00905451_m1), NFATc3 (Hs00190046_m1), NOS2 (Hs01075529_m1),* and *B2M* (Hs00187842_m1).

Spin column fractionation

The digested cell lysates were analysed using a modified MudPIT approach (Fränzel and Wolters 2011) (Washburn et al. 2001). Each protein digest was fractionated *via* strong cation exchange (SCX) using 4 mg polysulfoethyl A beads (PolyLC, Columbia MD) in 200 µL Eppendorf pipet tips. All spin column procedures were performed in a microcentrifuge at 2000 × *g* for 2 min. Briefly, SCX spin columns were washed twice with 100 µL SCX wash buffer (50 mM ammonium formate in 60% acetonitrile, pH 3). Protein digest samples were thawed and diluted 1:1 in binding buffer (50 mM ammonium formate in 10% acetonitrile, pH 3) and applied to the spin column. Peptide loaded SCX columns were washed twice with 200 µL SCX wash buffer. Fractionated peptides were sequentially eluted from the spin column using elution buffers of increasing strength (40, 80, 150, 500 mM ammonium formate in 10% acetonitrile, pH 3) and the final fraction eluted using a final elution buffer (500 mM ammonium formate in 5% acetonitrile, pH 5). Peptide fractions were eluted in clean, low-retention 1.5 mL siliconized microcentrifuge tubes. Solvent exchange was accomplished by evaporating eluted fractions to dryness in a Speedvac at room temperature and reconstituting each fraction in 65 µL 0.1% formic acid. Samples were maintained at 4 °C in the HPLC autosampler until analysed.

HPLC-MS/ms

Reversed-phase HPLC was performed using a Vanquish HPLC (Thermo Fisher Scientific, Waltham, MA) equipped with a 1 × 150 mm Hypersil GOLD™ C_{18} microbore column (Thermo Fisher Scientific, Waltham, MA) with a particle size of 1.9 µm. Peptides were eluted with a 100 µL/min gradient of 97/3 (A: 0.1% formic acid in water/B: 0.1% formic acid in acetonitrile) to 65/35 A/B over 60 min. The column temperature was maintained at 50 °C using an integrated column heater and interfaced to the mass spectrometer *via* positive electrospray ionisation using the HESI-II probe. Mass spectrometry analysis was performed using a Q-Exactive orbitrap mass spectrometer (Thermo Fisher Scientific, Waltham, MA) calibrated according to manufacturer's instructions using Tune (v2.9) instrument control software. The instrument was configured for data dependent analysis (DDA) using the full MS/DD-MS^2 (TopN) mode. Settings were as follows for MS^1 scans: Capillary spray voltage: 3.5 kV, heated capillary: 250 °C, auxiliary gas heater: 200 °C, sheath gas flow rate 35 arbitrary units, aux gas flow rate 10 arbitrary units, sweep gas flow rate 1 arbitrary unit, MS^1 resolution: 70 000 FWHM, MS^1 mass range: 200 – 2000 m/z, automatic gain control target: 3×10^6, injection time: 100 ms. Settings were as follows for MS^2 scans: Capillary spray voltage: 3.5 kV, heated capillary: 250 °C, auxiliary gas heater: 200 °C, sheath gas flow rate 35 arbitrary units, aux gas flow rate 10 arbitrary units, sweep gas flow rate 1 arbitrary

unit, MS^2 resolution: 17 500 FWHM, MS^2 mass range: 50 – 2000 m/z, automatic gain control target: 1×10^5, injection time: 100 ms, Isolation width: 4.0 *m/z*, N/CE: 30, TopN: 5, dynamic exclusion: 10 sec. Two technical replicates were performed for each digest fraction.

Statistical methods

Gene expression data was analysed and figures generated using GraphPad Prism 7.0 (GraphPad Software, La Jolla, CA, USA) using an unpaired t-test (two-tailed) and significance was applied using a threshold of $p < .05$ ($n = 4$ exp. and $n = 4$ non-exp). Proteomics data analysis was performed using a background-based t-test by Proteome Discoverer ($n = 9$ exp. and 8 non-exp). Significance was applied using a threshold of $p < 0.05$. For pathway analysis Reactome uses the Benjamini-Hochberg method for determining pathway over-representation. For the STRING tool analysis, a Fisher's exact test is used to generate a *p*-value indicating that the enrichment is unlikely to occur by chance.

Informatics

All raw MS spectra were analysed using Proteome Discoverer v2.5 protein informatics platform (Thermo Scientific, Waltham, MA). Mass spectrometry data was searched against the non-redundant *Homo sapiens* proteome (http://uniprot.org/proteomes/UP000005640 downloaded 06/24/2023) as well as an in-house maintained database of several hundred common proteomics contaminant proteins. Proteins were identified *via* the SEQUEST-HT algorithm using the following parameters: enzyme: trypsin, missed cleavages: 3 max, minimum peptide length: 6, precursor mass tolerance: 15 ppm, fragment mass tolerance: 0.2 Da, dynamic modifications: oxidation M, deamidation N, Q. Peptide validation was performed with the percolator node employing concatenated target/decoy selection, validation based on q value, and a target false discovery rate (FDR) of 0.01 for high confidence proteins and 0.05 for medium confidence proteins. Label-free quantitation was based on precursor intensity, using all unique peptides. Shared peptides were assigned using the razor approach.

Proteins or genes with statistically significant upregulation and detected in >75% of samples compared to non-exposed controls were selected for protein-protein interaction network analysis using the online STRING tool (Szklarczyk et al. 2021), and pathway analysis by Reactome.org. Accession numbers of the selected proteins or the gene symbol for upregulated genes were used for a database query of *Homo sapiens*

Results and discussion

RT-qPCR was used to quantify mRNA expression from cultured human keratinocytes among 39 candidate genes following MDI-GSH conjugate exposure or MDI-negative control. Of the 39 candidate genes surveyed, 9 exhibited significant upregulation following MDI-GSH exposure (Figure 1). A statistically significant ($p < 0.05$) increase in expression was detected for *NFATc2*, *PPARg*, *CXCL10*, *MCPIP*, *IL33*, *TSLP*, *GMCSF*, *CCL22*, and *IL1b*. The remaining 30 candidate genes either exhibited no significant change or were not detected (data not shown). The nine significantly upregulated genes are summarised in Table 1. The selected genes in this panel represent pathways related to adaptive immune responses and innate inflammatory responses that would indicate damage or dysfunction in the epidermal barrier. Specifically, the alarmins *IL33* and *TSLP* are important cytokines in both innate and adaptive immune

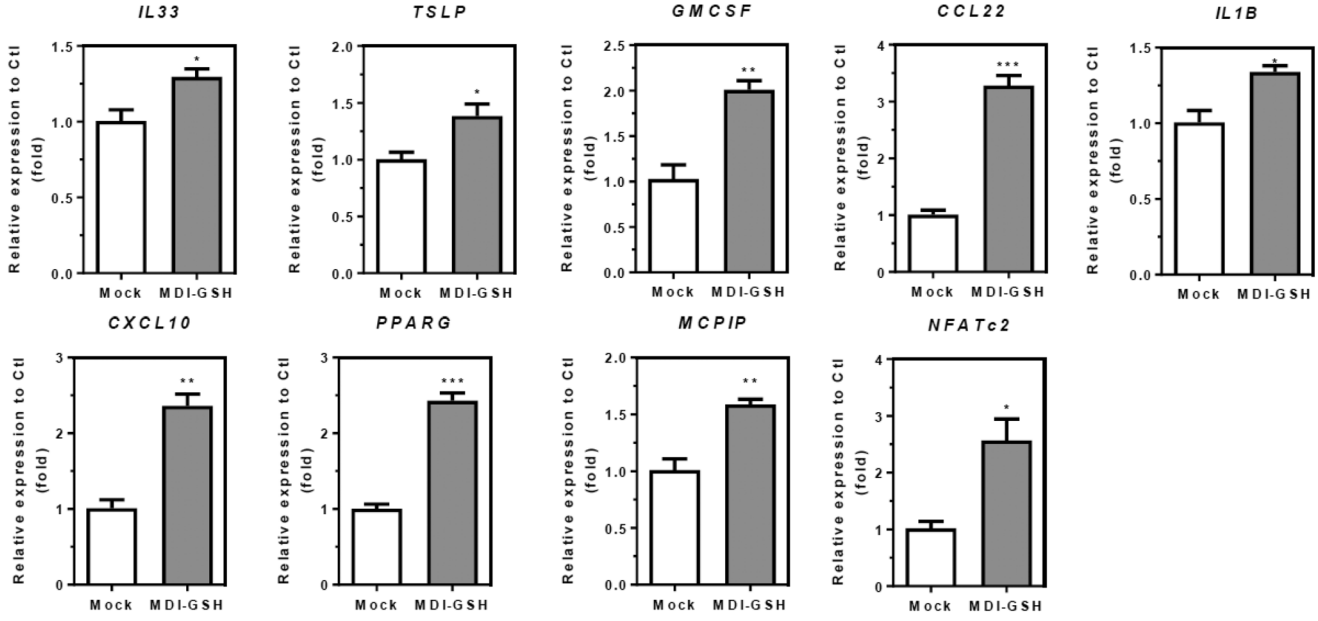

Figure 1. *In vitro* MDI-GSH conjugate exposure upregulates specific cytokines, chemokines, alarmins, and transcription factors in 24 h exposed cultured HEKa cells. Total RNA was isolated from cultured HEKa cells from either non-exposed (GSH only) or MDI-GSH exposed cells by *miRVana*™ miR isolation kit, reverse transcribed, and subjected to TaqMan RT-qPCR. Cytokines, chemokines, alarmins, and transcription factor mRNA expression of (A) *IL33,* (B) *TSLP,* (C) *GMCSF*, (D) *CCL22*, (E) *IL1B*, (F) *CXCL10*, (G) *PPARG*, (H) *MCPIP,* and (I) *NFATC2* were determined ($N = 7$; bars, s.e.m) (*$p < 0.05$, **$p < 0.01$, ***$p < 0.001$). Total RNA isolated from HEKa cells collected 24 h post-exposure to MDI-GSH conjugates in complete culture media exposure.

responses. The upregulation of these genes indicates that MDI-GSH exposure is resulting in the upregulation of alarmins indicating potential damage to the keratinocyte cell model. Increased expression of *IL1b*, *IL33* and *TSLP* can synergistically promote group 2 innate lymphoid cell (ILC2s) activation which can induce allergic and non-allergic inflammation, particularly in the skin and lungs (Toki et al. 2020; SH Lee et al. 2023). Increased expression of *GMCSF* and *CCL22* could attract T-cells to the site of an injury. *PPARg* has been indicated as a driving force in TH2 immune responses during nematode infection (Chen et al. 2017) and allergic disease by promoting the functions of ILC2s, M2 macrophages, and dendritic cells (Stark et al. 2021). All the aforementioned cytokines, chemokines, and alarmins play important roles in the TH2 immune response (Hasegawa et al. 2022). The roles of the other genes in Table 1 is less clear, however, *CXCL10* can attract T-cells, eosinophils, monocytes, and NK cells to sites of inflammation (Rohr et al. 2017) and *NFATc2* can be activated to modulate inflammatory responses.

Table 1. List of significantly upregulated genes in MDI-GSH/MDI exposed HEKa cells.

Gene symbol	Upregulation (fold change)	*p*-value	Role
IL33	1.3	0.0324	Alarmin
CCL22	3.28	0.0003	Chemokine
IL1B	1.34	0.0195	Cytokine
TSLP	1.38	0.0349	Alarmin
GMCSF	2.01	0.0063	Growth Factor
CXCL10	2.36	0.002	Chemokine
PPARG	2.43	0.0003	Transcription factor/ Regulator of Cutaneous Inflammation and Barrier Function
MCPIP	1.59	0.0059	Transcriptional activator/ endoribonuclease involved in mRNA decay/ Modulates the inflammatory response by degrading inflammation cytokines and chemokines
NFATc2	2.57	0.0176	Calcineurin/NFAT Signalling

Figure 2 presents the positive-ion electrospray mass spectrum obtained from the MDI-glutathione conjugation product. MS analysis of the conjugation product yields four major chemical species, including glutathione disulphide (GSSG, m/z 615.1754 u), the MDI-GSH conjugate (m/z 532.1866 u), reduced glutathione (GSH, m/z 308.0916 u), and 4,4′-methylenedianiline (MDA, 199.1235 u). Average mass accuracy across all peaks is 1.2 ppm. As can be seen in the mass spectrum, MDI may react with water, hydrolysing both isocyanate moieties to the amine forming non-reactive MDA; alternatively, one isocyanate moiety can react with the thiol of GSH to form the thiocarbamate while the second is hydrolysed to the amine. This species (m/z 532) may react further with protein *in vivo via* transcarbamoylation. To confirm the assignment of m/z 532, this reaction product was subjected to collision induced dissociation (CID) and tandem mass spectrometry in the orbitrap mass spectrometer. The fragment ion spectrum of the m/z 532 GSH-MDI conjugation product is presented in Figure 3. The m/z 532 product ion can be confidently assigned to MDI-GSH based on structurally relevant fragment ions. Ions produced from fragmentation of both glutathione (m/z 179, 233) and MDI (199, 225) are observed in the tandem mass spectrum of the MDI-GSH conjugate. Characterisation of the conjugation reaction products by mass spectrometry demonstrates the MDI-GSH conjugate formed under physiologically relevant conditions. No free isocyanate is observed in the reaction product, as it has been hydrolysed to the amine. This validates that HEKa cells were exposed to MDI in the form of MDI-GSH conjugate rather than free MDI.

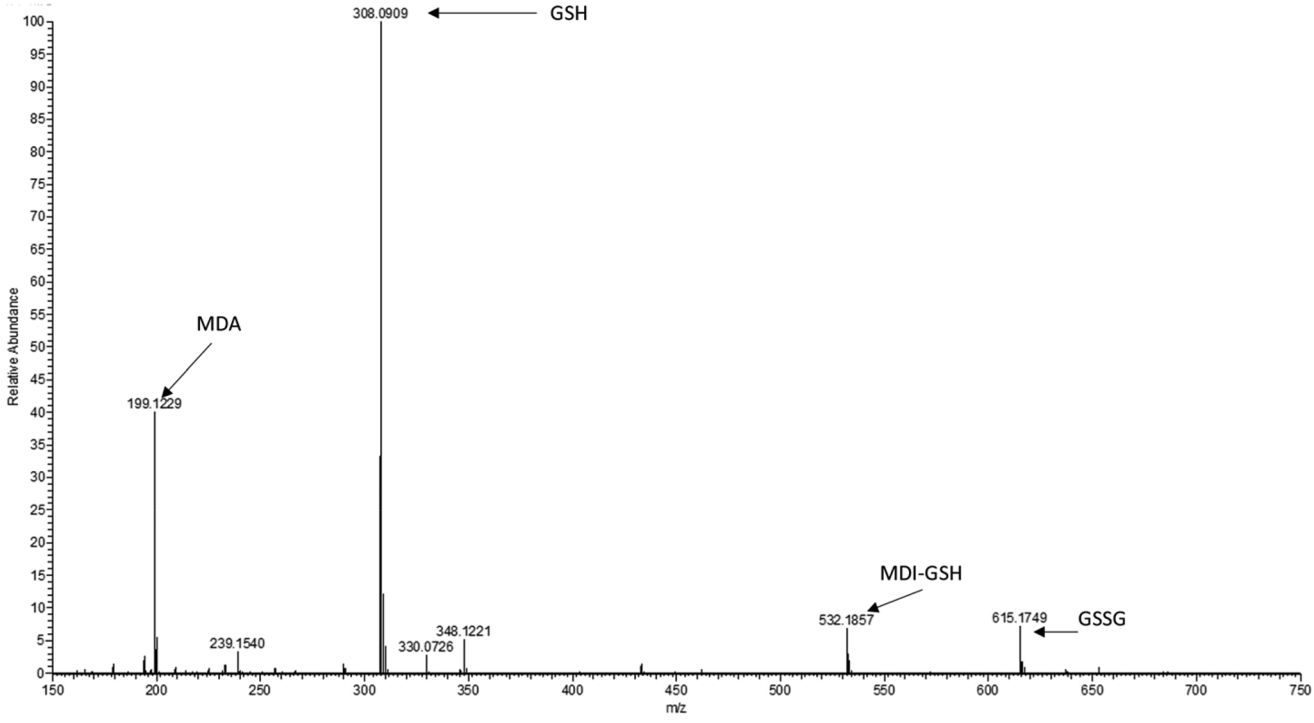

Figure 2. +ESI mass spectrum of the MDI-GSH conjugation reaction products.

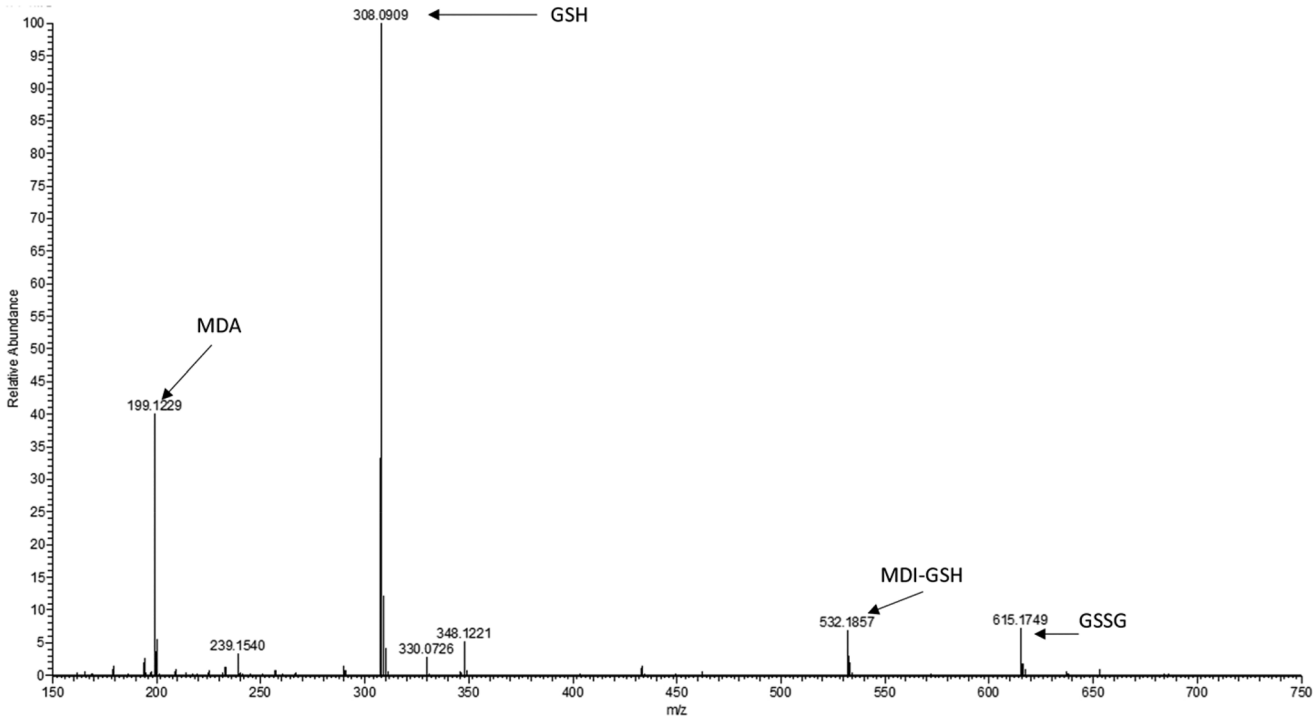

Figure 3. MS/MS analysis of m/z 532.1857 and predicted MS/MS fragments of MDI-GSH conjugate. Four predicted fragments were identified in the MS/MS of m/z 532.1857 including $[M+H]^+$ =179.0485, $[M+H]^+$=199.1228, $[M+H]^+$=225.1020, and $[M+H]^+$=233.0588.

Proteomics analysis of cultured human keratinocytes following MDI-GSH conjugate exposure or MDI-negative control was performed to determine protein identity and expression profiles. Off-line prefractionation of each cell lysate digest *via* strong cation exchange was performed prior to HPLC-MS/MS analysis. Five total fractions were obtained for each lysate digest, and the data recombined at the informatics stage. A summary of the full proteomics dataset has been uploaded (Supplementary Information, Table S1). In total, 18540 proteins were identified, and relative expression determined based on label-free quantitation across all samples based on 751559 peptide spectral matches (PSMs) (Supplementary Information, Table S2). Of the total 18540 identified proteins, 64 proteins exhibited statistically significant ($p<0.05$) changes in expression following MDI-GSH exposure. Proteins exhibiting up- and down-regulation following MDI-GSH conjugate exposure are listed in Tables 2 and 3, respectively. The dysregulated proteins identified in this dataset have been reported to participate in a range of immune and inflammatory pathways or are indicative of immune dysregulation. Among the dysregulated proteins, the protein S100A8/A9 heterodimer has been reported to participate in inflammatory pathways and may play a role in the development of MDI-OA. Increased expression of the protein S100A8/A9 heterodimer has been reported as an important damage associated molecular pattern molecule (DAMP)(S Wang et al. 2018). S100A8/A9 can act as a ligand for a variety of pattern recognition receptors (Turovskaya et al. 2008; Vogl et al. 2007) and can act as an endogenous ligand for toll-like receptor 4 (TLR4) and RAGE, both of which can trigger transcription factors such as NF-kB and AP-1 which are related to a variety of innate and adaptive immune processes downstream. Increased levels of S100A8/A9 have been noted in asthma, chronic obstructive pulmonary disease, acute respiratory distress syndrome, ventilator associated lung injury, and idiopathic pulmonary fibrosis (Prantner et al. 2020). In addition to increased expression of S100A8/A9, gene expression data provides evidence of the involvement of pattern recognition receptors RAGE and TLR4 (Table 2). Both are pattern recognition receptors that play a role in innate immune functions and act as a link between innate and adaptive immunity.

A multiomics approach was employed to consider both proteomic and gene expression datasets holistically. The online STRING protein association network tool was used to query the curated dataset of dysregulated proteins and genes to generate a protein-protein interaction map using the *Homo sapiens* database. STRING analysis ($p<0.005$) suggests three evident protein-protein interaction networks related to mRNA splicing, metabolic functions and pattern recognition receptors, NF-kB, MAPK signalling. Several pathways were significantly enriched, including those related to immune processes, pattern recognition receptors, protein synthesis, and metabolism. Protein and gene expression data was also merged and analysed using Reactome pathway analysis. Reactome Pathway Analysis showed a statistically significant overrepresentation for several pathways involved with inflammation and immune response using this protein expression data. These pathways included TLR functions by endogenous ligands, cytokine signalling, MyD88 pathways, EGFR activation, metal sequestration, antigen processing, cellular responses to stress, etc. Many of these pathways are highlighted in the analysis because of the upregulation of S100A8/A9, however, when this evidence is merged with the observed gene expression data, a clearer picture begins to emerge and support for upstream and downstream events related to inflammation, wound repair, and immune responses.

After exposing cultured HEKa cells to MDI-GSH conjugates proteomics and gene expression analysis was completed and

Table 2. List of the significantly upregulated quantified proteins in MDI-GSH/MDI exposed HEKa cells.

Protein description	Accession number (UniProt)	Fold change	*p*-value
ATP synthase subunit delta, mitochondrial	P30049	2.272	<0.001
ATP synthase subunit g, mitochondrial	O75964	1.603	0.010
Caveolae-associated protein 3	Q969G5	1.533	0.029
Complement component 1 Q subcomponent-binding protein, mitochondrial	Q07021	2.68	<0.001
Copine-9	Q8IYJ1	1.587	0.017
Cytochrome b-c1 complex subunit Rieske, mitochondrial	P47985	2.19	0.049
Cytochrome c oxidase subunit 5B, mitochondrial	P10606	3.51	<0.001
Density-regulated protein	O43583	1.631	0.017
Dynein light chain 1, cytoplasmic	P63167	5.439	<0.001
Far upstream element-binding protein 1	Q96AE4	2.275	<0.001
Fatty acid-binding protein 5	Q01469	1.635	<0.001
Galectin-7	P47929	2.596	<0.001
Hepatoma-derived growth factor	P51858	1.561	0.001
Heterogeneous nuclear ribonucleoprotein A1	P09651	1.826	<0.001
Heterogeneous nuclear ribonucleoproteins A2/B1	P22626	1.753	<0.001
High mobility group protein HMG-I/HMG-Y	P17096	2.445	<0.001
Histone-binding protein RBBP4	Q09028	3.292	0.005
Interleukin enhancer-binding factor 2	Q12905	1.795	0.042
Keratin, type I cytoskeletal 25	Q7Z3Z0	100	<0.001
Keratin, type I cytoskeletal 26	Q7Z3Y9	1.859	0.003
Non-histone chromosomal protein HMG-14	P05114	1.598	0.028
Nucleoside diphosphate kinase A	P15531	1.796	<0.001
Phosphoserine aminotransferase	Q9Y617	1.638	<0.001
Protein S100-A8	P05109	1.832	<0.001
Protein S100-A9	P06702	1.734	<0.001
Putative tubulin-like protein alpha-4B	Q9H853	100	<0.001
Ras-related protein Ral-A	P11233	3.118	0.001
Reticulocalbin-1	Q15293	2.076	<0.001
Suprabasin	Q6UWP8	4.011	<0.001
Translocator protein	P30536	1.602	0.001
Tubulin beta-2B chain	Q9BVA1	100	<0.001
Y-box-binding protein 3	P16989	1.624	0.003
Zinc finger protein 185	O15231	2.685	<0.001

Table 3. List of significantly downregulated quantified proteins in MDI-GSH/MDI exposed HEKa cells.

Description	Accession number (UniProt)	Fold change	*p*-value
Actin, aortic smooth muscle	P62736	0.515	0.004
CDP-diacylglycerol–inositol 3-phosphatidyltransferase	O14735	0.175	<0.001
Cornifin-B	P22528	0.49	0.048
D-dopachrome decarboxylase	P30046	0.442	0.038
EH domain-containing protein 3	Q9NZN3	0.357	0.005
Eukaryotic translation initiation factor 2 subunit 3B	Q2VIR3	0.102	<0.001
Guanine nucleotide-binding protein subunit beta-4	Q9HAV0	0.219	0.023
Hemoglobin subunit gamma-1	P69891	0.339	0.017
High mobility group protein B1	P09429	0.432	0.015
Histidine–tRNA ligase, mitochondrial	P49590	0.027	<0.001
Integrin alpha-2	P17301	0.488	0.011
Integrin alpha-V	P06756	0.522	0.050
Keratin, type II cytoskeletal 72	Q14CN4	0.435	0.016
Keratin-like protein KRT222	Q8N1A0	0.367	<0.001
Lactadherin	Q08431	0.178	0.002
Laminin subunit beta-3	Q13751	0.498	0.001
Macrophage migration inhibitory factor	P14174	0.48	0.017
N-chimaerin	P15882	0.57	0.034
Parathymosin	P20962	0.33	<0.001
Prohibitin-2	Q99623	0.397	<0.001
Protein transport protein Sec61 subunit alpha isoform 1	P61619	0.323	<0.001
Putative annexin A2-like protein	A6NMY6	0.01	<0.001
Ras-related protein Rab-4B	P61018	0.01	<0.001
Retinoic acid-induced protein 3	Q8NFJ5	0.136	<0.001
Small ribosomal subunit protein eS4, Y isoform 1	P22090	0.281	0.007
Small ribosomal subunit protein eS4, Y isoform 2	Q8TD47	0.184	0.001
Sulfide:quinone oxidoreductase, mitochondrial	Q9Y6N5	0.557	0.029
Transmembrane protein 40	Q8WWA1	0.496	0.023

compared to unexposed cultured cells. Several differences in protein expression were observed between the exposed and control groups. Proteomic analysis showed an up-regulation of protein S100A8 and S100A9, an important alarmin, and normally heterodimeric protein, that can act as an endogenous ligand for several pattern recognition receptors important to both innate and adaptive immune responses. Increased expression of *IL33* can lead to the increased release of the alarmins S100A8 and S100A9 (proteomics) and downstream *TSLP* (gene expression), these pathways have been shown to promote inflammation and both have been found in patients with airway inflammatory responses and patients with autoimmune disease (Kato et al. 2017). Increased expression of *TSLP* and *IL33* has been shown to synergistically enhance each other's release in lung epithelium and enhance the activation of group 2 innate lymphoid cells (ILC2) in the lung airway epithelium (Shin et al. 2019). Evidence now suggests that ILCs play a role in the development of asthma with or without adaptive immune responses (Mirchandani et al. 2014; Oliphant et al. 2011; Neill and Flynn 2018; Kim et al. 2016) which could help explain the absence of a specific IgE in some MDI-OA patients.

Although ILC2s do mirror functions of T-cells, they do not express antigen receptors or clonal selection/expansion (Eberl et al. 2015). ILC2s do react rapidly to signals from infected and injured tissues (Spits and Mjösberg 2022; Vivier et al. 2018). Interestingly, it has been reported that ILC2s may play an important role in pulmonary barrier dysfunction after lung injury leading to an upregulation on M2 type macrophages. Recently, M2 macrophage gene signatures and endogenous murine M2 marker mRNAs have been observed in mice after exposure to MDI-GSH conjugates (Wisnewski et al. 2015; 2020). Our lab has recently confirmed the presence of M2 markers, transcription factors, and chemokines in MDI-GSH exposed murine macrophages (Lin et al. 2023). This could offer insight to a connection between a dermal exposure to MDI and MDI-OA. Previous studies have reported increased ILC2s in the peripheral blood of patients with allergic diseases such as asthma (Bartemes et al. 2014). Recent studies have shown activation induced migration of ILC2s (Kim et al. 2016) and that ILC2s could mediate inflammatory events in two different organs and connections between allergic diseases (Johansson Mali'n et al. 2014). Further studies are required to explore this potential link.

In addition to increased expression of S100A8, S100A9. *TSLP*, and *IL33*, expression changes were observed involving other barrier proteins, immune proteins, alarmins, proteins involved with metabolism, and proteins that may indicate

inflammation or oxidative stress. These discoveries, and observed gene expression changes, make for a strong case that pattern recognition receptors such as TLR's or RAGE and ILC2s might be involved in the pathogenesis of MDI-OA.

Asthma is a complex lung disease that can result from an adaptive immune response to a specific antigen (extrinsic asthma) or by other, non-allergic, inflammatory responses (intrinsic asthma). MDI-OA is often associated with a history of dermal MDI exposure (Liljelind et al. 2010); however, only a minority of MDI-OA patients exhibit specific IgE antibodies to MDI. When considering dermal exposure as a potential route of entry into the body, the role of keratinocytes must be considered. Keratinocytes are known to play an important role in activation of adaptive and innate immune responses when the dermal barrier is challenged by pathogens or toxins. Glutathione, an important biological antioxidant, is also relevant in dermal exposures due to its presence in the epidermal barrier. Glutathione is present in all animal cells at concentrations of 0.5 – 10 mmol/L. Studies have confirmed reactions between glutathione and dNCOs do indeed occur (Wisnewski et al. 2013; 2015; Johansson Mali'n et al. 2014). Furthermore, human proteins can undergo transcarbamoylation *via* MDI-GSH and it has been hypothesised that cell membrane proteins may be targets and evoke downstream inflammatory events (Wisnewski et al. 2013; 2015). The differential protein expression data reported in this manuscript support the hypothesis that keratinocytes have the capacity to react to insult by MDI-GSH conjugates.

When considering the evidence, it is a safe assumption that inflammation, innate, and adaptive immune pathways are involved with MDI-OA. Published data suggests that dermal exposure to MDI should be considered an important, if not pivotal, event for development of the disease. Airborne concentrations of MDI in industry are well controlled, thanks in part to MDI's physiochemical properties. The absence of respirable MDI points to the skin as the next likely route of entry, and both human and animal studies have shown that dermal exposures lead to sensitisation. This hypothesis is further supported by the increased use of less volatile MDI without an appreciable decrease in occupational asthma with a history of isocyanate exposure (Booth et al. 2009; Henriks-Eckerman et al. 2015). It is therefore logical to explore potential mechanisms within the dermal barrier including its predominant cell type, the keratinocyte. Keratinocytes are known to be important to wound healing, inflammation, and adaptive immune responses. Keratinocytes express pattern recognition receptors and are capable of producing DAMPs, cytokines, and chemokines in response to injury or assault (Yousef et al. 2024). The keratinocyte response to MDI-GSH exposure should offer insights into downstream pathways. Our lab has also demonstrated that conditioned media from keratinocytes exposed to MDI-GSH conjugate elicits chemoattraction of lymphocytes (data not shown), further evidence that the confluent cell model does, in fact, react in an immunologic way under these exposure conditions.

Conclusion

Occupational asthma following exposure to MDI continues to be an important, and ever-growing problem with the increasing demand of urethane coatings, adhesives, and foam products. The protein and gene expression data we report here suggests that MDI exposure may activate pathways in either extrinsic or intrinsic type asthma. We have identified dysregulated proteins in keratinocytes exposed to MDI-GSH conjugates that participate in barrier integrity, innate immune pathways, adaptive immune pathways, and inflammatory pathways. When considering our observations, the diversity of MDI-OA in patients, and previously reported evidence, it is doubtful that a single group of pathways (adaptive immunity, innate immunity, or inflammatory) will emerge to explain the pathogenesis of MDI-OA. The data reported in this manuscript suggests a complex interplay of multiple pathways and potential outcomes, most likely influenced by individual genotypes and phenotypes resulting in the pathogenesis of MDI-OA. However, this data does suggest a reason to further explore epidermal barrier integrity and immune/inflammatory responses after exposure to MDI-GSH. Future studies will include exploring putative pathways and signalling related to the activation of immune and inflammatory regulators like NF-kB and AP-1, as well as studies into the potential role of ILC2s in the pathogenesis of MDI-OA. Although not proven definitively, when considering industrial hygiene data showing very low airborne concentrations in most industrial settings, it is evident that skin exposures to MDI probably play an important role in the development of MDI-OA in many cases. The data presented in this report supports previous studies that indicate that exposures and the biological processes underlying the development of MDI-OA are complex. Previously published data and sampling data suggested that MDI skin exposure and penetration of the dermis probably play an important role in the development of MDI-OA. When considering that approximately 90% of the epidermis is composed of keratinocytes and their importance in alerting and activating immune responses, it would be remiss to not assess a potential role in MDI exposure and participation in the development of MDI-OA. The data reported in this manuscript suggests a mixture of innate and adaptive immune responses being activated or dysregulated 24 hrs following MDI-GSH conjugate exposure in keratinocytes. The authors acknowledge that additional doses, exposure paradigms and time points will be required to elucidate specific pathways which influence the ultimate biological, and specifically immunological, fate of MDI in the skin. However, this data does imply, under these specific conditions and dose, a dermal exposure to MDI-GSH conjugate has the potential to elicit immune responses and inflammation that could lead to immunologic memory and inflammatory responses compatible with the development of MDI-OA.

Disclosure statement

The authors declare that they have no conflicting financial interests. The findings and conclusions in this report are those of the authors and do not necessarily represent the official position of the National Institute for Occupational Safety and Health, Centres for Disease Control and Prevention. All data used in the preparation of this manuscript is publicly available on the NIOSH Data and Statistics Gateway (https://www.cdc.gov/niosh/data/researchdata.html).

Funding

This work was supported by intramural funds (CAN#19390BN8 and #39390KK5) from the National Institute for Occupational Safety and Health, Centres for Disease Control and Prevention.

ORCID

Brandon F. Law http://orcid.org/0000-0002-3658-6547
Chen-Chung Lin http://orcid.org/0000-0001-5686-2169
Justin M. Hettick http://orcid.org/0000-0002-9143-1513

References

Balmes J, Becklake M, Blanc P, Henneberger P, Kreiss K, Mapp C, Milton D, Schwartz D, Toren K, Viegi G, et al. 2003. American Thoracic Society Statement: occupational contribution to the burden of airway disease. Am J Respir Crit Care Med. 167:787–797.

Bartemes KR, Kephart GM, Fox SJ, Kita H. 2014. Enhanced innate type 2 immune response in peripheral blood from patients with asthma. J Allergy Clin Immunol. 134(3):671.e4–678.e4. doi: 10.1016/j.jaci.2014.06.024.

Bernstein DI, Korbee L, Stauder T, Bernstein JA, Scinto J, Herd ZL, Bernstein IL. 1993. The low prevalence of occupational asthma and antibody-dependent sensitization to diphenylmethane diisocyanate in a plant engineered for minimal exposure to diisocyanates. J Allergy Clin Immunol. 92(3):387–396. doi: 10.1016/0091-6749(93)90117-x.

Bernstein IL. 1999. Asthma in the workplace. New York: M. Dekker.

Blanc PD, Toren K. 1999. How much adult asthma can be attributed to occupational factors? Am J Med. 107(6):580–587. doi: 10.1016/s0002-9343(99)00307-1.

Booth K, Cummings B, Karoly WJ, Mullins S, Robert WP, Spence M, Lichtenberg FW, Banta J. 2009. Measurements of airborne methylene diphenyl diisocyanate (MDI) concentration in the U.S. workplace. J Occup Environ Hyg. 6(4):228–238. doi: 10.1080/15459620902724060.

Bowler RP, Crapo JD. 2002. Oxidative stress in allergic respiratory diseases. J Allergy Clin Immunol. 110(3):349–356. doi: 10.1067/mai.2002.126780.

Chen T, Tibbitt CA, Feng X, Stark JM, Rohrbeck L, Rausch L, Sedimbi SK, Karlsson MCI, Lambrecht BN, Karlsson Hedestam GB, et al. 2017. PPAR-γ promotes type 2 immune responses in allergy and nematode infection. Sci Immunol. 2(9):eaal5196. doi: 10.1126/sciimmunol.aal5196.

Chieosilapatham P, Kiatsurayanon C, Umehara Y, Trujillo-Paez JV, Peng G, Yue H, Nguyen LTH, Niyonsaba F. 2021. Keratinocytes: innate immune cells in atopic dermatitis. Clin Exp Immunol. 204(3):296–309. doi: 10.1111/cei.13575.

Dewitte JD, Chan-Yeung M, Malo JL. 1994. Medicolegal and compensation aspects of occupational asthma. Eur Respir J. 7(5):969–980.

Eberl G, Colonna M, Di Santo JP, McKenzie AN. 2015. Innate lymphoid cells. Innate lymphoid cells: a new paradigm in immunology. Science. 348(6237):aaa6566. doi: 10.1126/science.aaa6566.

Engfeldt M, Isaksson M, Zimerson E, Bruze M. 2013. Several cases of work-related allergic contact dermatitis caused by isocyanates at a company manufacturing heat exchangers. Contact Dermatitis. 68(3):175–180. doi: 10.1111/j.1600-0536.2012.02167.x.

Fränzel B, Wolters DA. 2011. Advanced MudPIT as a next step toward high proteome coverage. Proteomics. 11(18):3651–3656. doi: 10.1002/pmic.201100056.

Hasegawa T, Oka T, Demehri S. 2022. Alarmin cytokines as central regulators of cutaneous immunity. Front Immunol. 13:876515. doi: 10.3389/fimmu.2022.876515.

Henriks-Eckerman ML, Mäkelä EA, Laitinen J, Ylinen K, Suuronen K, Vuokko A, Sauni R. 2015. Role of dermal exposure in systemic intake of methylenediphenyl diisocyanate (MDI) among construction and boat building workers. Toxicol Lett. 232(3):595–600. doi: 10.1016/j.toxlet.2014.12.012.

Intelligence M. 2023. Methylene diphenyl diisocyanate (MDI) market size & share analysis- growth trends & forecast EMIS. Mordor Intelligence. https://www.mordorintelligence.com/industry-reports/methylene-diphenyl-di-isocyanate-mdi-market.

Janssen-Heininger YM, Poynter ME, Aesif SW, Pantano C, Ather JL, Reynaert NL, Ckless K, Anathy V, van der Velden J, Irvin CG, et al. 2009. Nuclear factor kappaB, airway epithelium, and asthma: avenues for redox control. Proc Am Thorac Soc. 6(3):249–255. doi: 10.1513/pats.200806-054RM.

Jiang Y, Tsoi LC, Billi AC, Ward NL, Harms PW, Zeng C, Maverakis E, Kahlenberg JM, Gudjonsson JE. 2020. Cytokinocytes: the diverse contribution of keratinocytes to immune responses in skin. JCI Insight. 5(20):e142067. doi: 10.1172/jci.insight.142067.

Johansson Mali'n T, Lindberg S, Åstot C. 2014. Novel glutathione conjugates of phenyl isocyanate identified by ultra-performance liquid chromatography/electrospray ionization mass spectrometry and nuclear magnetic resonance. J Mass Spectrom. 49(1):68–79. doi: 10.1002/jms.3306.

Kato T, Kouzaki H, Matsumoto K, Hosoi J, Shimizu T. 2017. The effect of calprotectin on TSLP and IL-25 production from airway epithelial cells. Allergol Int. 66(2):281–289. doi: 10.1016/j.alit.2016.06.011.

Kim HY, Umetsu DT, Dekruyff RH. 2016. Innate lymphoid cells in asthma: will they take your breath away? Eur J Immunol. 46(4):795–806. doi: 10.1002/eji.201444557.

Lambrecht BN, Hammad H. 2015. The immunology of asthma. Nat Immunol. 16(1):45–56. doi: 10.1038/ni.3049.

Lee CT, Ylostalo J, Friedman M, Hoyle GW. 2005. Gene expression profiling in mouse lung following polymeric hexamethylene diisocyanate exposure. Toxicol Appl Pharmacol. 205(1):53–64. doi: 10.1016/j.taap.2004.09.015.

Lee SH, Kang B, Kamenyeva O, Ferreira TR, Cho K, Khillan JS, Kabat J, Kelsall BL, Sacks DL. 2023. Dermis resident macrophages orchestrate localized ILC2 eosinophil circuitries to promote non-healing cutaneous leishmaniasis. Nat Commun. 14(1):7852. doi: 10.1038/s41467-023-43588-2.

Liljelind I, Norberg C, Egelrud L, Westberg H, Eriksson K, Nylander-French LA. 2010. Dermal and inhalation exposure to methylene bisphenyl isocyanate (MDI) in iron foundry workers. Ann Occup Hyg. 54(1):31–40. doi: 10.1093/annhyg/mep067.

Lin CC, Law BF, Hettick JM. 2023. 4,4′-Methylene diphenyl diisocyanate exposure induces expression of alternatively activated macrophage-associated markers and chemokines partially through Krüppel-like factor 4 mediated signaling in macrophages. Xenobiotica. 53(12):653–669. doi: 10.1080/00498254.2023.2284867.

Lin CC, Liu LZ, Addison JB, Wonderlin WF, Ivanov AV, Ruppert JM. 2011. A KLF4-miRNA-206 autoregulatory feedback loop can promote or inhibit protein translation depending upon cell context. Mol Cell Biol. 31(12):2513–2527. doi: 10.1128/MCB.01189-10.

Lofgren DJ, Walley TL, Peters PM, Weis ML. 2003. MDI exposure for spray-on truck bed lining. Appl Occup Environ Hyg. 18(10):772–779. doi: 10.1080/10473220301441.

Maestrelli P, Boschetto P, Fabbri LM, Mapp CE. 2009. Mechanisms of occupational asthma. J Allergy Clin Immunol. 123(3):531–542; quiz 43-4. doi: 10.1016/j.jaci.2009.01.057.

Malo JL, Chan-Yeung M. 2009. Agents causing occupational asthma. J Allergy Clin Immunol. 123(3):545–550. doi: 10.1016/j.jaci.2008.09.010.

Mirchandani AS, Besnard AG, Yip E, Scott C, Bain CC, Cerovic V, Salmond RJ, Liew FY. 2014. Type 2 innate lymphoid cells drive CD4+ Th2 cell responses. J Immunol. 192(5):2442–2448. doi: 10.4049/jimmunol.1300974.

Neill DR, Flynn RJ. 2018. Origins and evolution of innate lymphoid cells: wardens of barrier immunity. Parasite Immunol. 40(2):e12436. doi: 10.1111/pim.12436.

NIOSH. 1994a. Letter from NIOSH to Distinctive Designs International Inc with a study report. Cincinnati (OH): US Department of Health and Human Services, Public Health Service, Centers for Disease Control, National Institute for Occupational Safety and Health.

NIOSH 1994b. Letter from NIOSH to Jim Walter Resources, Inc with a study report. Cincinnati (OH): US Department of Health and Human

Services, Public Health Service, Centers for Disease Control, National Institute for Occupational Safety and Health.

Oliphant CJ, Barlow JL, McKenzie AN. 2011. Insights into the initiation of type 2 immune responses. Immunology. 134(4):378–385. doi: 10.1111/j.1365-2567.2011.03499.x.

Piipponen M, Li D, Landén NX. 2020. The immune functions of keratinocytes in skin wound healing. Int J Mol Sci. 21(22):8790. doi: 10.3390/ijms21228790.

Prantner D, Nallar S, Vogel SN. 2020. The role of RAGE in host pathology and crosstalk between RAGE and TLR4 in innate immune signal transduction pathways. FASEB J. 34(12):15659–15674. doi: 10.1096/fj.202002136R.

Rahman I, MacNee W. 2002. Oxidative stress and adaptive response of glutathione in bronchial epithelial cells. Clin Exp Allergy. 32(4):486–488. doi: 10.1046/j.0954-7894.2002.01368.x.

Redlich CA, Karol MH. 2002. Diisocyanate asthma: clinical aspects and immunopathogenesis. Int Immunopharmacol. 2(2-3):213–224. doi: 10.1016/s1567-5769(01)00174-6.

Rohr M, Oleinikov K, Jung M, Sandjo LP, Opatz T, Erkel G. 2017. Anti-inflammatory tetraquinane diterpenoids from a Crinipellis species. Bioorg Med Chem. 25(2):514–522. doi: 10.1016/j.bmc.2016.11.016.

Shin JI, Lee KH, Joo YH, Lee JM, Jeon J, Jung HJ, Shin M, Cho S, Kim TH, Park S, et al. 2019. Inflammasomes and autoimmune and rheumatic diseases: a comprehensive review. J Autoimmun. 103:102299. doi: 10.1016/j.jaut.2019.06.010.

Spits H, Mjösberg J. 2022. Heterogeneity of type 2 innate lymphoid cells. Nat Rev Immunol. 22(11):701–712. doi: 10.1038/s41577-022-00704-5.

Stark JM, Coquet JM, Tibbitt CA. 2021. The role of PPAR-γ in allergic disease. Curr Allergy Asthma Rep. 21(11):45. doi: 10.1007/s11882-021-01022-x.

Szklarczyk D, Gable AL, Nastou KC, Lyon D, Kirsch R, Pyysalo S, Doncheva NT, Legeay M, Fang T, Bork P, et al. 2021. The STRING database in 2021: customizable protein-protein networks, and functional characterization of user-uploaded gene/measurement sets. Nucleic Acids Res. 49(D1):D605–D612. doi: 10.1093/nar/gkaa1074.

Toki S, Goleniewska K, Zhang J, Zhou W, Newcomb DC, Zhou B, Kita H, Boyd KL, Peebles RS. 2020. TSLP and IL-33 reciprocally promote each other's lung protein expression and ILC2 receptor expression to enhance innate type-2 airway inflammation. Allergy. 75(7):1606–1617. doi: 10.1111/all.14196.

Turovskaya O, Foell D, Sinha P, Vogl T, Newlin R, Nayak J, Nguyen M, Olsson A, Nawroth PP, Bierhaus A, et al. 2008. RAGE, carboxylated glycans and S100A8/A9 play essential roles in colitis-associated carcinogenesis. Carcinogenesis. 29(10):2035–2043. doi: 10.1093/carcin/bgn188.

Vivier E, Artis D, Colonna M, Diefenbach A, Di Santo JP, Eberl G, Koyasu S, Locksley RM, McKenzie ANJ, Mebius RE, et al. 2018. Innate lymphoid cells: 10 years on. Cell. 174(5):1054–1066. doi: 10.1016/j.cell.2018.07.017.

Vogl T, Tenbrock K, Ludwig S, Leukert N, Ehrhardt C, van Zoelen MA, Nacken W, Foell D, van der Poll T, Sorg C, et al. 2007. Mrp8 and Mrp14 are endogenous activators of Toll-like receptor 4, promoting lethal, endotoxin-induced shock. Nat Med. 13(9):1042–1049. doi: 10.1038/nm1638.

Wang J-N, Li M. 2020. The immune function of keratinocytes in anti-pathogen infection in the skin. Int J Dermatol Venereol. 3(4):231–238. doi: 10.1097/JD9.0000000000000094.

Wang S, Song R, Wang Z, Jing Z, Wang S, Ma J. 2018. S100A8/A9 in inflammation. Front Immunol. 9:1298. doi: 10.3389/fimmu.2018.01298.

Washburn MP, Wolters D, Yates JR.3rd. 2001. Large-scale analysis of the yeast proteome by multidimensional protein identification technology. Nat Biotechnol. 19(3):242–247. doi: 10.1038/85686.

Wass U, Belin L. 1989. Immunologic specificity of isocyanate-induced IgE antibodies in serum from 10 sensitized workers. J Allergy Clin Immunol. 83(1):126–135. doi: 10.1016/0091-6749(89)90487-9.

Wisnewski AV, Cooney R, Hodgson M, Giese K, Liu J, Redlich CA. 2022. Severe asthma and death in a worker using methylene diphenyl diisocyanate MDI asthma death. Am J Ind Med. 65(3):166–172. doi: 10.1002/ajim.23323.

Wisnewski AV, Liu J, Colangelo CM. 2015. Glutathione reaction products with a chemical allergen, methylene-diphenyl diisocyanate, stimulate alternative macrophage activation and eosinophilic airway inflammation. Chem Res Toxicol. 28(4):729–737. doi: 10.1021/tx5005002.

Wisnewski AV, Liu J, Redlich CA. 2013. Connecting glutathione with immune responses to occupational methylene diphenyl diisocyanate exposure. Chem Biol Interact. 205(1):38–45. doi: 10.1016/j.cbi.2013.06.005.

Wisnewski AV, Liu J, Redlich CA. 2020. Analysis of lung gene expression reveals a role for Cl(-) channels in diisocyanate-induced airway eosinophilia in a mouse model of asthma pathology. Am J Respir Cell Mol Biol. 63(1):25–35. doi: 10.1165/rcmb.2019-0400OC.

Wisnewski AV, Liu Q, Miller JJ, Magoski N, Redlich CA. 2002. Effects of hexamethylene diisocyanate exposure on human airway epithelial cells: in vitro cellular and molecular studies. Environ Health Perspect. 110(9):901–907. doi: 10.1289/ehp.02110901.

Wisnewski AV, Stowe MH, Cartier A, Liu Q, Liu J, Chen L, Redlich CA. 2004. Isocyanate vapor-induced antigenicity of human albumin. J Allergy Clin Immunol. 113(6):1178–1184. doi: 10.1016/j.jaci.2004.03.009.

Ye YM, Kim CW, Kim HR, Kim HM, Suh CH, Nahm DH, Park HS, Redlich CA, Wisnewski AV. 2006. Biophysical determinants of toluene diisocyanate antigenicity associated with exposure and asthma. J Allergy Clin Immunol. 118(4):885–891. doi: 10.1016/j.jaci.2006.06.026.

Yousef H, Alhajj M, Sharma S. 2024. Anatomy, skin (integument), epidermis. Treasure Island (FL): StatPearls Publishing